Adsorbate-induced surface stress, surface strain and surface reconstruction: S on Cu(100) and Ni(100)

M.K. Bradley, D.P. Woodruff* and J. Robinson

Physics Department, University of Warwick, Coventry CV4 7AL, UK

Abstract

Density Functional Theory (DFT) calculations have been applied to investigate the known difference in behaviour of S adsorption on Cu(100) and Ni(100). Both surfaces form a 0.25 ML (2x2) adsorption phase, but while at higher coverage a 0.5 ML c(2x2) phase forms on Ni(100), on Cu(100) only a reconstructed 0.47 ML (√17x√17)R14° structure occurs. Calculations of the energy, structure, and surface stress of (2x2) and c(2x2) phases on both substrates show there is an energy advantage on both surfaces to form the higher coverage phase, but that both surfaces show local surface strain around the S atoms in the (2x2) phase, a phenomenon previously investigated only on Cu(100). More than forty different structural models of the Cu(100)(√17x√17)R14°-S phase have been investigated. The pseudo-(100)c(2x2) structure previously proposed, containing 16 Cu adatoms per unit mesh in the reconstructed layer, is found to be less energetically favourable than many other possible structures, even after taking account of local structural relaxations. Significantly more favourable is a structure with 12 Cu adatoms per (√17x√17)R14° unit mesh, previously proposed on the basis of scanning tunnelling microscopy (STM), and found to yield simulated STM images in good agreement with experiment. This model has all S atoms in local 4-fold coordinated hollows relative to the Cu atoms below, half being located above Cu adatoms with the remainder lying above the underlying outermost substrate layer. However, an alternative model with only 4 Cu adatoms and with half the S atoms at 3-fold coordinated sites on the periphery of the Cu adatom cluster, has an even lower energy and gives simulated STM images in excellent agreement with experiment.

---

* corresponding author. email d.p.woodruff@warwick.ac.uk

1. Introduction

While early studies of adsorption on single-crystal surfaces tended to regard the substrate as a rigid atomic chequer-board upon which atoms and molecules adsorb, it is now well-established that such adsorption invariably causes some structural modification of the underlying surface. In some cases, the resulting changes are quite subtle, involving small local atomic relaxations, but in others major reconstruction of the surface occurs. While the structure that results is (in the absence of kinetic constraints) the one with the lowest free energy, one component of the total energy, namely the surface stress, is often invoked to explain particular adsorbate-induced surface structural changes.

One of the very few cases for which there appears to be experimental evidence for adsorbate-induced lateral strain without major reconstruction is in the Cu(100)(2x2)-S surface, with several independent investigations indicating that the four surface Cu atoms surrounding the S atoms adsorbed in hollow sites are displaced radially outwards from the S atom by approximately 0.03 Å [1, 2, 3, 4]. A further interesting feature of the Cu(100)/S system is the significant difference in behaviour relative to the Ni(100)/S system. Atomic S forms stable (2x2) phases on both Cu(100) and Ni(100) [5] at a coverage of 0.25 ML, but the 0.5 ML c(2x2) phase that forms on Ni(100) [6] is not seen on Cu(100); as the surface strain around the adsorbed S atom that is possible in the (2x2) phase becomes symmetry forbidden in the c(2x2) phase, it is tempting to suggest that a higher S-induced compressive stress on Cu(100) may be the cause of this difference. In fact a high-coverage (0.47 ML) S phase is found on Cu(100)/S, but this is associated with a reconstructed ($\sqrt{17}$x$\sqrt{17}$)R14° phase [7]. No quantitative structure determination exists for this structure, but one suggested model [8] comprises a (100)-like c(2x2) reconstructed layer that has Cu-Cu distances 3% larger than those of the underlying (rotated) Cu(100) substrate. This model is quite similar to the one originally proposed by Domange and Oudar [7], based on the formation of a Cu_2S compound layer. Of course, while Cu and Ni are both fcc solids with lattice parameters that differ by only ~2%, their electronic and chemical properties differ considerably. Nevertheless, the observed local surface strain in the Cu(100)(2x2)-S phase, and the fact that the high-coverage phase may

involve a strained reconstructed layer, does suggest that adsorbate-induced compressive surface stress may be an important factor on this surface.

In order to investigate these similarities and differences, and to try to establish the structure of the Cu(100)(√17x√17)R14°-S phase, we have undertaken a density functional theory (DFT) investigation of the interaction of S with Cu(100) and Ni(100) surfaces. In particular, we have evaluated the relative total energies and surface stresses in different structural models, and compare the lowest-energy structures of the Cu(100)(√17x√17)R14°-S phase with the results of a scanning tunnelling microscopy (STM) investigation of this phase [9].

2. Computational Details

The DFT calculations reported here were conducted using the plane-wave pseudopotential computer code CASTEP 5.501 [10]. The RPBE exchange-correlation functional [11] was used in the majority of the calculations along with ultrasoft pseudopotentials, although a few comparative calculations were performed using the PBE functional [12]. These two functionals are generally regarded as well-suited for investigations of metals. A plane wave cutoff energy of 360 eV was found to provide adequate basis set convergence, although a slightly higher value of 400 eV was used for copper for compatibility with calculations on another adsorption system not reported here. A relatively dense Monkhorst-Pack k-point mesh (16x16x1 k-points) was needed, along with a Hellmann-Feynman force tolerance of 0.01 eV/Å, to provide well-converged surface stresses in the double-sided 9-layer surface slabs considered in the calculations based on a (2x2) mesh. The inner-most three layers were constrained to the bulk metal structure found in the DFT calculations with lattice parameters for Cu and Ni of 3.6658 Å and 3.5794 Å, respectively. Using these values to define the lateral dimensions of the slabs ensures that there is zero lateral stress in the 'bulk'. Initial calculations using the (√17x√17) unit mesh were on 4-layer single-sided slabs (3 bulk layers plus an outer reconstructed surface layer) using Hellmann-Feynman force tolerance of 0.02 eV/Å and 4x4x1 k-points, although some of the most favourable structures were then investigated

using 9-layer slabs as used for the (2x2) mesh calculations. A vacuum gap of at least 14 Å was used to ensure minimal interaction between slabs. Calculations of the total energy of the S_2 free molecule, used to provide a reference for the adsorption energies, were performed in a 10x10x12 $Å^3$ cell. Alternative references, such as S atoms in H_2S, would change the absolute adsorption energies per atom, but have no effect on their relative values, although this change would affect E^* values for structures with different coverages.

The adsorption energy per S atom on the double-sided slabs was determined from

$$E_a = -\frac{1}{2N_S}\left(E_{substrate+S} - E_{substrate} - N_S E_{S_2}\right)$$

where N_S is the number of S atoms in the unit mesh (on each side of the slab), $E_{substrate+S}$ is the total energy of the slab for the adsorption system, $E_{substrate}$ is the total energy for the clean surface slab, and E_{S_2} is the energy of an isolated S_2 molecule. Notice that this definition leads to a positive value of E_a for stable adsorption, so the larger values correspond to stronger bonding. However, in order to compare the total energy reduction associated with structures having different surface coverages it is helpful to define an effective surface energy change which we label E_a^*, defined for the double-sided slabs as

$$E_a^* = -\frac{\left(E_{substrate+S} - E_{substrate} + 2(17 - N_{metal})E_{bulk-metal} - N_S E_{S_2}\right)}{A}$$

and for single-sided slabs as

$$E_a^* = -\frac{\left(E_{substrate+S} - E_{substrate} + (17 - N_{metal})E_{bulk-metal} - \frac{1}{2}N_S E_{S_2}\right)}{A}$$

This definition also allows for structures in the outermost layer comprising not only N_S adsorbed S atoms per surface unit mesh, but also N_{metal} metal atoms, as in the models of the Cu(100)(√17x√17)R14°-S phase in which the number of Cu atoms in the reconstructed surface is less than the 17 Cu atoms found in each of the bulk layers. For these structures $E_{substrate+S}$ consisted of three (or seven) bulk layers plus the reconstructed layer, whereas $E_{substrate}$ was a 4-layer (or 9-layer) clean surface slab, so the third term in the equation corrects the energy for the 'missing' number of Cu surface atoms (17-N_{metal}).

A is the area of the surface (or surfaces in the case of the double-sided slab) in units of the area of the (1x1) mesh of the clean unreconstructed surface.

For the double-sided slabs, in which each face has an identical adsorbate coverage, leading to the same surface stress on each face, and it is particularly trivial to extract the value of the surface stress from the calculated three-dimensional stress tensor, computed within CASTEP according to the so-called stress theorem [13].

3. Results

3.1 (2x2) calculations on Cu(100) and Ni(100)

We first consider the relative surface energies and surface stresses associated with the known (2x2)-S phase on both Ni(100) and Cu(100), the known c(2x2)-S structure on Ni(100), and the Cu(100)c(2x2)-S phase which does not occur in practice. The key results are summarised in Table 1. Notice that the calculated isotropic tensile surface stress values (the surfaces are 4-fold symmetric, so S_x=S_y) for the clean surfaces of Ni(100) and Cu(100) are in excellent agreement with the previously-reported values by Harrison *et al*. [14] of 2.22 N/m and 1.89 N/m, respectively. The calculated compressive stress induced by 0.5 ML of S adsorption on Ni(100) of -0.13 N/m is significantly smaller, however, than that reported by Harrison *et al.* (-0.98 N/m). This is most probably attributable to the fact that the PBE functional used in these earlier calculations is known to bond adsorbates more strongly than the RPBE function used here; a new PBE calculation for the Cu(100)c(2x2)-S structure similarly yielded a compressive stress 0.65 N/m larger in magnitude than that shown in Table 1 from the RPBE calculation (see Table 4). In the case of the Ni(100)c(2x2)-S surface there is actually an experimental measurement of the adsorbate-induced *change* in the surface stress of -5.0 N/m [15, 16], which is significantly larger than the value found in the present calculations (-2.42 N/m) or in the earlier calculations on Harrison *et al.* (-3.21 N/m). This earlier publication [14] highlights significant differences (both larger and smaller) between experimental and theoretical adsorbate-induced surface stress changes and discusses some possible causes.

The calculated structural values are in excellent agreement with experimental values where these exist. For Ni(100) the S-Ni outermost layer spacings, $z_{Ni\text{-}S,}$ were found in the experiments to be 1.30±0.10 Å for both the c(2x2) [6] and (2x2) phases [5]. Reported experimental values for $z_{Cu\text{-}S}$ in the Cu(100)(2x2)-S phase of 1.28±0.03 Å [1], 1.19±0.14 Å [2], 1.30±0.05 Å [3] and 1.32±0.03 Å [4] are all slightly smaller than our calculated value, but after taking account of the experimental error estimates the last two values are fully consistent with the DFT result while the discrepancies with the first two values are only 0.04 Å and 0.02 Å. The calculated lateral outward shift of the nearest-neighbour Cu atoms to the S adsorbates, Δ_{xy}, is also in excellent agreement with the values reported in these same four experimental studies which all fall in the narrow range 0.03-0.04 Å (despite precision values that are mostly greater than 0.01 Å). One interesting conclusion of our calculations is that a similar local distortion of Δ_{xy}=0.03 Å should occur in the Ni(100)(2x2)-S structure; there appears to have been no experimental investigation of this possibility.

In truth, there is rather little in the results of Table 1 to suggest that a c(2x2)-S phase should not form on Cu(100). Clearly it is still energetically favourable for S to be adsorbed onto the (2x2)-S phase; the calculated adsorption energy per S atom in a c(2x2) phase, E_a, is lower than in the (2x2) phase, as is also the case on Ni(100), but the energy gain per unit area of surface, as reflected in E_a*, is larger. On both metal surfaces, S adsorption at a coverage of 0.25 ML leads to reduction in the tensile surface stress of the clean surface, while further adsorption to a coverage of 0.5 ML leads to the surface stress becoming compressive. The compressive stress calculated for the Cu(100)c(2x2)-S phase is significantly larger than for the equivalent phase on Ni(100), but the total energy change clearly favours this higher coverage. It is notable, though, that the increase in E_a* in going from the (2x2) to c(2x2) phase is much smaller on Cu(100) than on Ni(100) (perhaps related to the difference in compressive surface stress), rendering it more likely that a high-coverage reconstructed phase might be preferred on the copper surface.

In view of the fact that no Cu(100)c(2x2)-S phase at a coverage of 0.5 ML actually occurs in practice, but that the 0.47 ML Cu(100)(√17x√17)R14°-S structure forms

instead, we infer that this reconstruction must lead to a lower total energy. We have therefore investigated possible structural models of this phase. Of course, this much larger surface mesh is more computationally demanding, which is why we have concentrated initially on calculations based on a smaller 4-layer one-sided slab. The main disadvantage of using a single-sided slab is that it is no longer straightforward to extract the surface stress values, because the slab now has different stresses on its two faces and we calculate only the total stress on the asymmetric slab. It is also possible that the total energy changes associated with the adsorption structures are no longer exactly comparable with those of the (2x2)-phase calculations based on the nine-layer double-sided slabs. However, the relative energies of different structural models of the (√17x√17) should be rather reliable. The subsequent 9-layer calculations of the most favoured structures address these limitations.

The earlier-proposed structural models of this structure, based on a Cu_2S compound layer, or a pseudo-(100)c(2x2)-S overlayer, both have a surface phase comprising 16 Cu atoms and 8 S atoms (coverage 0.47 ML) per surface mesh, to be compared with 17 Cu atoms in the underlying layers of the bulk Cu. The main difference seems to be that the Cu_2S compound was described as a two-dimensional layer, implying coplanar Cu and S atoms, whereas the pseudo-(100)c(2x2)-S layer was envisaged as involving a chemisorbed S overlayer. This latter model is shown in Fig. 1, together with a similar diagram of the relaxed version of this structure obtained from the DFT energy minimisation (model A in Table 2). A range of additional possible structures were investigated, mainly characterised by different numbers of Cu and S atoms per surface unit mesh. Table 2 lists the energy gain per (1x1) unit mesh of surface, E_a*, and the stress values of these alternative structures. Also included in Table 2 are values of the slab stress on a clean unreconstructed Cu(100) surface calculated using the same 4-layer slab and the same (√17x√17) unit mesh. Because both faces of this slab are unconstrained in layer spacings and have the same (zero) adsorbate coverage, this is effectively a double-sided slab, so the slab stress value of 2.70 N/m equates to a clean surface stress of 1.35 N/m. The difference between this value and that obtained from the nine-layer slab using a (2x2) mesh (2.06 N/m) can be attributed to the differences in slab thickness and k-point

sampling. A calculation using the (√17x√17) unit mesh in a double-sided 9-layer slab yields a value of 1.80 N/m (Table 3), the smaller difference from the value in the (2x2) mesh now being entirely attributable to the differences in k-point sampling.

Table 2 summarises the main features of a range of different structural models tested using the 4-layer slab calculations. In most of these structures the S coverage of 8/17 ML has been used, consistent with the experimental value obtained by a novel radiotracer technique by Domange and Oudar [7], but the number of Cu atoms in the unit mesh has been varied, while for a given number of Cu and S atoms in the unit mesh, different assumptions regarding their location in the starting model has led to different local energy minima with different structures. These tests were very extensive, but it is impossible to be sure that they are 100% inclusive . The lowest energy structure found in these calculations, corresponding to the largest value of E_a*, is model N, and this is shown in Fig. 2. A key difference from the pseudo-(100)c(2x2) structure is that rather than there being 16 Cu atoms per unit mesh in the reconstructed surface, there are only 12. As a result, there is considerably more space for the Cu atoms to arrange themselves and the result is that half of the S atoms occupy a layer above these Cu atoms, but half bond to the underlying unreconstructed surface. An interesting feature of this model is that all the S atoms, as in the pseudo-(100)c(2x2) structure, occupy 4-fold coordinated hollow sites relative to the Cu atoms below, although the S atoms that bond to the underlying substrate are each sufficiently close to two Cu adatoms that they are actually 6-fold coordinated and form slightly shorter bonds to the adatoms (2.33 Å and 2.37 Å)) than to the substrate atoms below (2.42-2.49 Å). The shortest Cu-S bonds are those formed by the S atoms that lie above, and are 4-fold coordinated to, the groups of four Cu adatoms (2.22-2.35 Å). This structural model is essentially that proposed by Colaianni and Chorkendorf [9] in their STM study of the surface, with only small local relaxations in the atomic positions; as these authors suggested, this model can account for the STM images they observed. In particular, the S atoms above the Cu adatoms are much higher above the surface and correlate with the protrusion tetramers seen in the STM. Fig. 3 shows a comparison of their reported STM image with a simulated image (based on the standard Tersoff and Hamann [17] approach) obtained from the DFT calculations on

model N.

One notable feature of Table 2 is that the E_a* values all fall in quite a narrow range (0.142 eV) of energies with Model A being the least favourable and model N the most favourable. It is therefore important to stress that this mode of expressing the energy difference, per (1x1) surface unit mesh, is one reason for the differences being so small. For example, if one were to quote the total energy per (√17x√17) unit mesh, the energy range would be 17 times larger (2.41 eV), while even quoting the energies per adsorbed S atom corresponds to an increase of a factor of 2.13 for all those structure having a S coverage of 8/17 ML. A detailed discussion of all the alternative models of Table 2 seems inappropriate, but we should perhaps comment on model I which corresponds to the same coverage of Cu adatoms and S adsorbate atoms as the pseudo-(100)c(2x2) structure of model A. These two structures differ in E_a* by a rather significant value of 55meV or 40% of the full energy range of the models, so one might ask "what is the structural difference?" In fact the key difference is that the Cu atoms in model I effectively occupy two different layers, allowing some S atoms to bond to the underlying substrate. In this sense, therefore, the structure also has features in common with the most favourable model N.

While the fact that structural model N is the most energetically favourable of all the models tested (E_a*=0.952 eV, Table 2), and is clearly consistent with STM images recorded from the Cu(100)(√17x√17)R14°-S surface, it is notable that a c(2x2)-S structure is, according to our calculations, more energetically favoured (E_a*=0.967 eV, Table 1). Clearly this is inconsistent with the experimental evidence that a c(2x2)-S phase never forms on Cu(100). On the basis that this inconsistency may be due in large part to the differences in slab thickness, new 9-layer slab calculations were performed in the (√17x√17) mesh for both the clean surface and structure N. The results are included in Table 3. In fact the new surface energy gain per (1x1) mesh for model N is now E_a*=0.929 eV, 23 meV less than in the 4-layer calculations and 38 meV less than the c(2x2) phase, a result which is even less consistent with experiment.

In view of this some further exploration of alternative structural models was investigated, using the 9-layer slab calculations. The main results are summarised in Table 3, although a further 22 structures (not shown in Table 3) were also tested using a smaller (2x2x1) density of k-point sampling in order to try to identify promising new structural models. Two new models, model R and model V, proved to be more energetically favourable than model N, and are illustrated in Fig. 4. In model R the 4-fold rotational symmetry on model N is retained, and the key difference is that the number of Cu adatoms per unit mesh is reduced from 12 to 4; in model N 4 of the 8 S atoms per unit mesh lie in 4-fold coordinated hollows on the Cu adatoms and are 1.58 Å higher on the surface than the remaining S atoms that are bound to the underlying Cu atoms of the unreconstructed surface. As may be expected, the STM image is dominated by these outermost S atoms. In model R the number of Cu atoms per unit mesh is reduced to 4, and the STM image is dominated by the 4 S atoms that lie at the periphery of these squares of Cu atoms; the height difference between these S atoms and those on the underlying surface that are not bonded to Cu adatoms is reduced to 0.88 Å. Notice that these S atoms are only 3-fold coordinated to Cu atoms, lying essentially atop Cu atoms in the underlying surface. Inspection of the range of structures investigated indicates that there appears to be no very significant difference in the total of energy of structures involving different numbers of 3-fold and 4-fold coordinated S atoms; in particular, the preference for 4-fold coordination assumed in the original rationalisation of the pseudo-square reconstruction does not seem to be correct.

One structural difference between model N and model R, which leads to a difference in the simulated STM images, is that the lateral separation of the raised S atoms is smaller in model N (3.90 Å) than in model R (4.32 Å), so the separation of the STM protrusions within the tetramers differs relative to their spacing. Quantitative comparison with the experimental STM image is difficult, however, due to noise and some distortion of the images; the comparison appears to favour model R, but the achievable precision is marginal.

While the experimental STM images are clearly dominated by the tetramer groups that

appear to be approximately 4-fold symmetric, it does seem that the uppermost protrusion of each group is somewhat larger and brighter that the other three, leading to the possibility that there may be an intrinsic asymmetry. Model V shows one way in such an asymmetry can be introduced. This model has six Cu adatoms per unit mesh, such that one S atom occupies a 4-fold coordinated hollow above these adatoms (as in model N), while three S atoms occupy sites at the periphery of the Cu adatom clusters (as in model R). A simulated STM image from this structure is shown in Fig. 4, but although this does show the qualitative asymmetry that appears to be present in the experimental image, the quantitative agreement is clearly poor. The S atom above the Cu atoms lies almost exactly 1.0 Å above those at the periphery of the Cu adatom cluster, so this is not really surprising. While the calculations show model V to be favoured over model R by 20 meV per (1x1) mesh, this comparison of the STM images seems to show rather clearly that model V does not correspond to the true surface structure. Of course, the reduced symmetry of model V means that there are many more structural parameters to optimise and in theoretical fitting of experimental data it is generally found that increasing the number of parameters leads to improved fits that are not necessarily physically meaningful. There seems no reason, however, for this argument to be applicable to the DFT structure determination, and indeed we have found that if calculations of a symmetric structure are conducted with the usual symmetry constraints relaxed, no significant energy reduction is achieved.

The other outstanding problem with these results is that the lowest energy reconstruction model that is compatible with the experimental STM images (model R) is still less favourable that a simple c(2x2) overlayer structure by 25 meV per (1x1) mesh, yet this c(2x2) structure is never observed. One possible source of this discrepancy is that the k-point sampling of (√17x√17)R14° structure must necessarily be different from that of a (2x2) mesh as used for the c(2x2)-S structure. Generally, in comparing energies of this type, it is important to use the same unit mesh and k-point sampling, but c(2x2) is not a submesh of (√17x√17)R14°, so this is not possible. However, calculations for the clean unreconstructed surface using the two different meshes show a difference of only 3 meV/(1x1) mesh, indicating that the k-point sampling in both meshes is sufficiently

dense for this to lead to only very small discrepancies. One further test of the general reliability of the results is to compare the energies of the different structures using a different functional, and for this purpose new calculations of the main structural models of interest were performed (using 9-layer double-sided slabs) using the PBE functional. The results are shown in Table 4. These calculations show much smaller energy differences between Models N, R and V (a range of only 8 meV/(1x1) mesh) with model N now favoured over model R, but model V still has the lowest energy. As in the RPBE calculations, however, the c(2x2) structure is still favoured over these reconstruction models by 30-40 meV/(1x1) mesh.

4. Conclusions

In the (2x2) structures formed on both Ni(100) and Cu(100) by 0.25 ML atomic S, the results of our DFT calculations show excellent agreement with experimentally-measured structural parameters including, in the case of the Cu(100)(2x2)-S phase, the small lateral outwards strain of the four Cu atoms neighbouring the S adsorbate atoms. Our calculations also show that this same strain should occur on the Ni(100)(2x2)-S surface, although this possibility has not been investigated experimentally. Consistent with this is the fact that our calculations show a large reduction in the surface tensile stress of the surface in the presence of this S coverage. Increasing the S coverage to 0.5 ML to produce a c(2x2) phase leads to this surface stress becoming slightly compressive on Ni(100), and strongly compressive on Cu(100). The much larger compressive stress in the case of the Cu(100)c(2x2)-S structure is consistent with the idea that this may provide a rationale as to why this simple phase does not form, but instead a (√17x√17)R14° construction occurs on Cu(100) at a saturation coverage of 0.47 ML. However, ultimately it is the minimisation of the total (free) energy, and not the surface stress, that determines the equilibrium structure.

Extensive tests of different structural models of the Cu(100)(√17x√17)R14°-S phase reveal a number of features. Firstly, optimisation of the strained pseudo-(100) [8] (or equivalently, the Cu_2S surface sulphide model [7]), in which the reconstructed layer

contains 16 Cu atoms and 8 S atoms per unit mesh (model A), shows that there is very significant relaxation of the Cu atom positions in this reconstructed layer relative to their positions in the simple model. More significantly, an alternative model (model N) involving 12 Cu 'adatoms' in the surface layer, leading to tetramers of raised S atoms, as originally proposed on the basis of STM images [9], is very significantly favoured energetically over model A by ~140 meV/(1x1) unit mesh. Calculations for more than 40 different structural models, involving particularly different numbers of Cu atoms within the reconstructed layer, show that several structures have rather similar total energies, and that the exact relative energies of the most favourable structures are dependent on the DFT functional used in the calculations. However, only two of these structures, that originally proposed in the experimental STM study (model N) and a variant of this with a much lower Cu adatom coverage (model R), appear to be consistent with the experimentally-observed STM images. These models involve significant differences in the S-Cu layer spacings and so should be readily distinguished by a number of standard quantitative surface structural techniques such as low energy electron diffraction, photoelectron diffraction, or X-ray standing waves.

One outstanding puzzle is that that none of these structural models have a lower total energy in our calculations than a c(2x2)-S phase, a structure that is not observed experimentally. Coincidentally, we also note that the lowest energy structure, (by 20 meV/(1x1) mesh in RPBE) is incompatible with the experimental STM images. The energy differences involved (≥~25 meV/(1x1) unit mesh, or ≥~50 meV/S atom between model R and the c(2x2) phase) may be due to the need to perform the comparative calculations using different surface mesh sizes, although simple tests on the clean surface suggest that the resultant error should be much smaller than this, so the origin of this discrepancy remains unclear.

Tables

Substrate	Cov. {S} (ML)	Phase	E_a (eV)	E_a* (eV)	S_x(surf)= S_y (surf) (Nm^{-1})	$z_{M\text{-}S}$ (Å)	Δ_{xy} (Å)
Ni(100)	0	clean	-	-	2.29	-	-
Ni(100)	¼	p(2x2)	3.282	0.820	1.46	1.28	0.03
Ni(100)	½	c(2x2)	2.913	1.456	-0.13	1.30	-
Cu(100)	0	clean	-	-	1.91	-	-
Cu(100)	¼	p(2x2)	2.475	0.619	1.28	1.35	0.03
Cu(100)	½	c(2x2)	1.933	0.967	-1.67	1.34	-

Table 1. Summary of the main results of the calculations of surface energy, surface stress, and local geometry for S adsorption on Cu(100) and Ni(100) in (2x2) and c(2x2) unit meshes.

Cu coverage (ML)	S coverage (ML)	Structural model	E_a* (eV)	S_x (slab) (Nm^{-1})	S_y (slab) (Nm^{-1})
16/17	8/17	A♦	0.810	1.03	1.03
15/17	8/17	B	0.864	0.53	0.84
16/17	8/17	C	0.818	0.76	0.77
14/17	8/17	D	0.858	0.98	0.87
13/17	8/17	E	0.811	0.63	0.91
12/17	8/17	F	0.823	0.83	0.79
11/17	8/17	G	0.859	0.84	0.93
11/17	8/17	H	0.870	0.46	0.74
16/17	8/17	I	0.865	0.94	1.22
12/17	12/17	J♦	0.813	0.65	0.65
12/17	10/17	K♦	0.871	0.66	0.66
12/17	11/17	L♦	0.918	0.57	0.57
12/17	10/17	M♦	0.931	0.74	0.74
12/17	8/17	N♦	0.952	1.28	1.28
13/17	8/17	O♦	0.892	1.31	1.31
13/17	8/17	P	0.884	1.58	1.58
unreconstructed	0	clean	-	2.70	2.70

Table 2 Calculated surface energies and stresses for different structural models of the Cu(100)(√17x√17)R14°-S structure using the 4-layer slabs. Models denoted ♦ are 4-fold symmetric, so S_x=S_y. Note that the stress values S_x and S_y relate to the complete one-sided slab with different surface stresses on each side. The qualitative changes in these values are attributable to changes in the surface stress on the adsorbate-covered face, but no attempt is made to separate the contributions of the two faces.

Cov. {Top Cu layer (ML)	Cov. {S} (ML)	Phase	E_a* per (1×1) (eV)	S_x (Nm^{-1})	S_y (Nm^{-1})
12/17	8/17	N♦	0.929	0.44	0.44
8/17	8/17	Q♦	0.920	-0.66	-0.66
4/17	8/17	R♦	0.942	-0.40	-0.40
5/17	8/17	S♦	0.896	0.09	0.09
0/17	8/17	T♦	0.792	0.94	0.94
2/17	8/17	U	0.830	-0.13	-0.49
6/17	8/17	V	0.962	0.22	-0.21
unreconstructed	0	clean		1.80	1.80

Table 3 Calculated surface energies and stresses for further structural models of the Cu(100)(√17x√17)R14°-S structure using the double-sided 9-layer slabs. Models denoted ♦ are 4-fold symmetric, so S_x=S_y.

Cov. {Top Cu layer (ML)	Cov. {S} (ML)	Phase	E_a* per (1×1) (eV)	S_x (Nm^{-1})	S_y (Nm^{-1})
12/17	8/17	N	1.067	0.06	0.06
4/17	8/17	R	1.062	-0.73	-0.73
6/17	8/17	V	1.070	-0.03	-0.46
c(2x2)	1/2	c(2x2)	1.103	-2.32	-2.32

Table 4 Calculated surface energies and stresses for the three principal models of the Cu(100)(√17x√17)R14°-S structure and for the Cu(100)c(2x2)-S structure using double-sided 9-layer slabs and the PBE functional.

Figure Captions

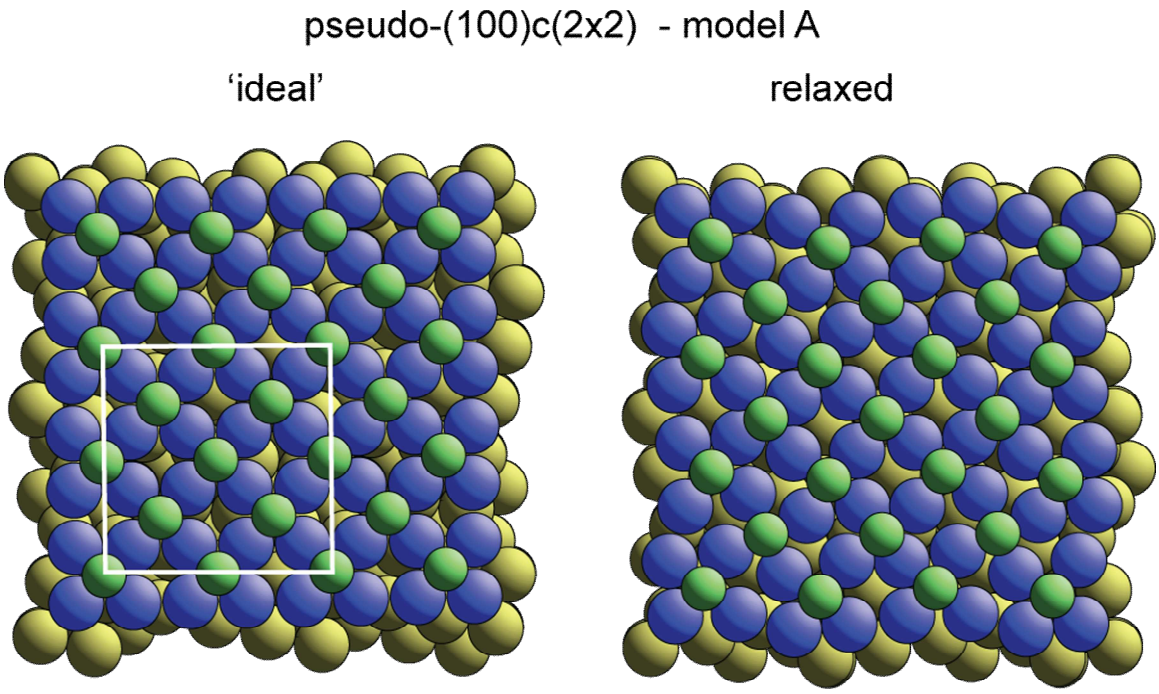

Fig. 1 Plan view of the 'ideal' and relaxed versions of the pseudo-(100)c(2x2) model of the Cu(100)(√17x√17)R14°-S structure. The white square shows the unit mesh. For clarity the Cu atoms in the outermost (reconstructed) layer are shown in a different colour (blue) than the underlying bulk atoms (yellow/gold). The S atoms are represented by the smaller (green) spheres.

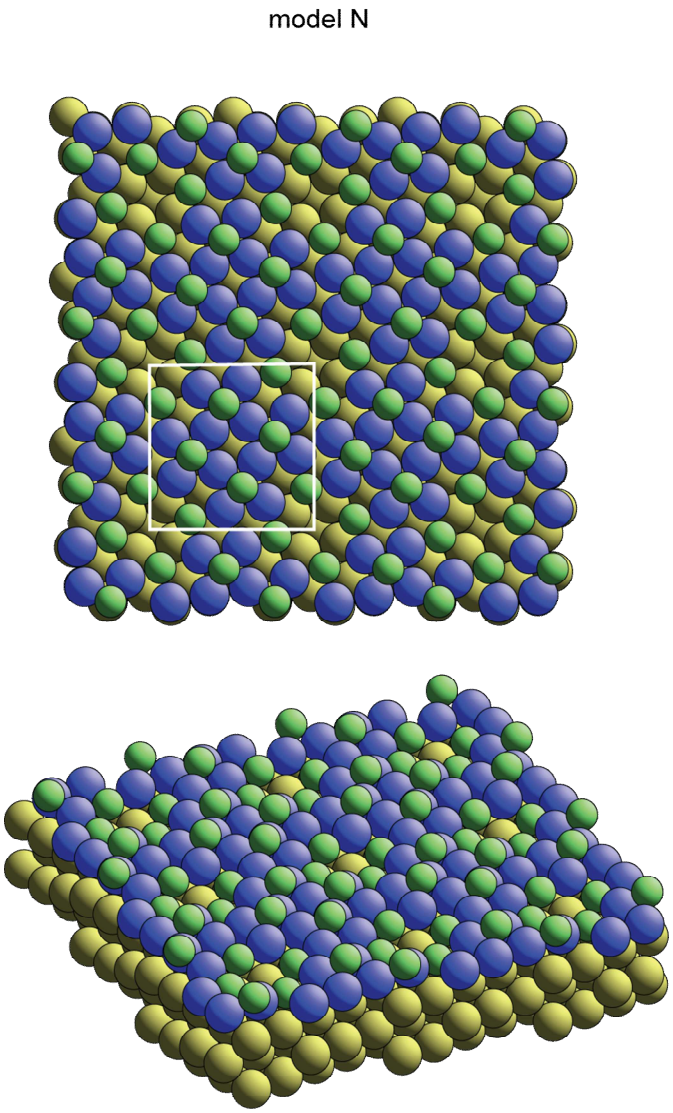

Fig. 2 Plan and perspective views of model N of the Cu(100)(√17x√17)R14°-S structure. The white square shows the unit mesh. For clarity the Cu atoms in the outermost (reconstructed) layer are shown in a different colour (blue) than the underlying bulk atoms (yellow/gold). The S atoms are represented by the smaller (green) spheres.

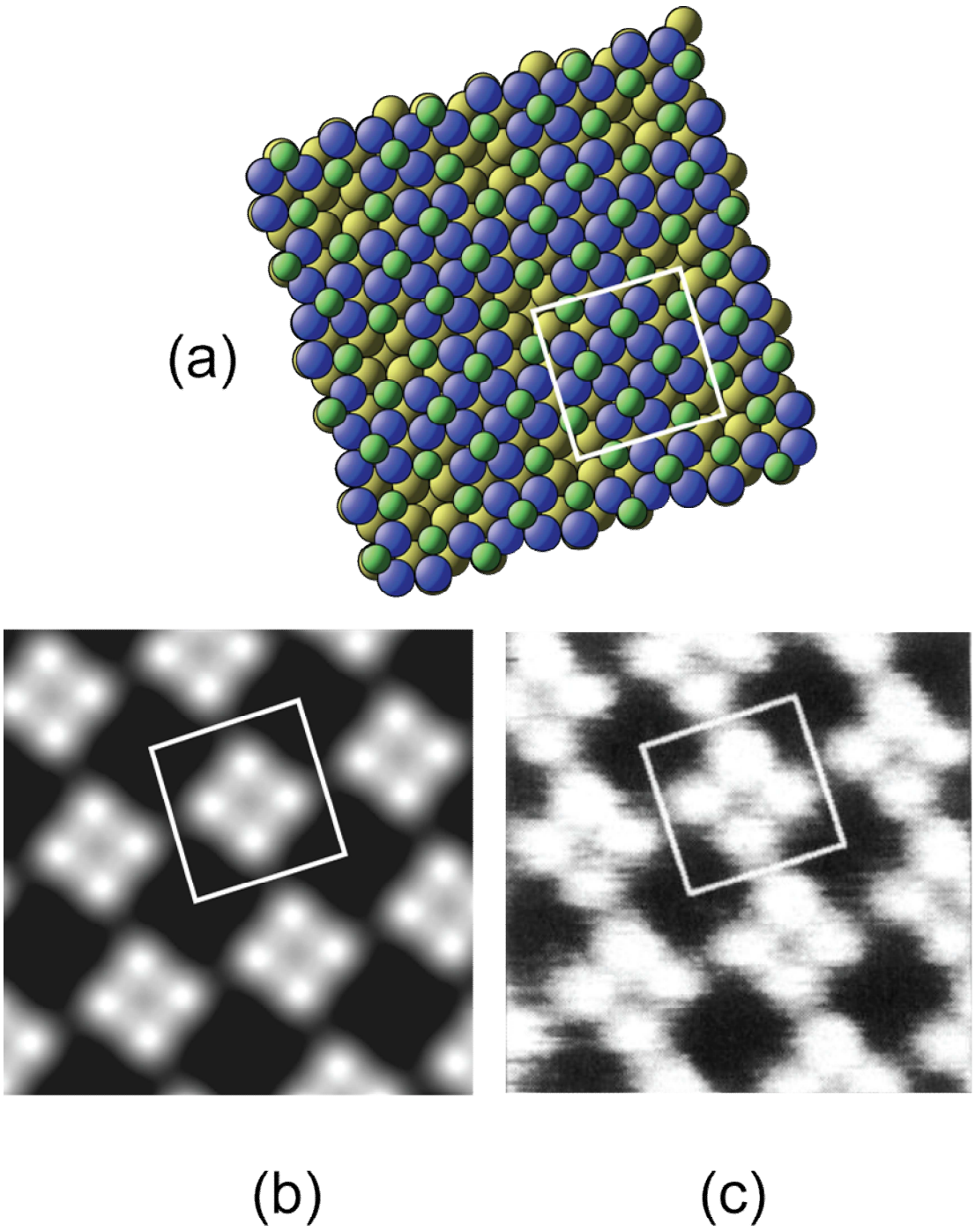

Fig. 3 Comparison the experimental [9] (c) and simulated (b) STM images from the Cu(100)(√17x√17)R14°-S surface. The simulations are based on the model structure N (Fig. 2) shown in its mirror reflection domain (a).

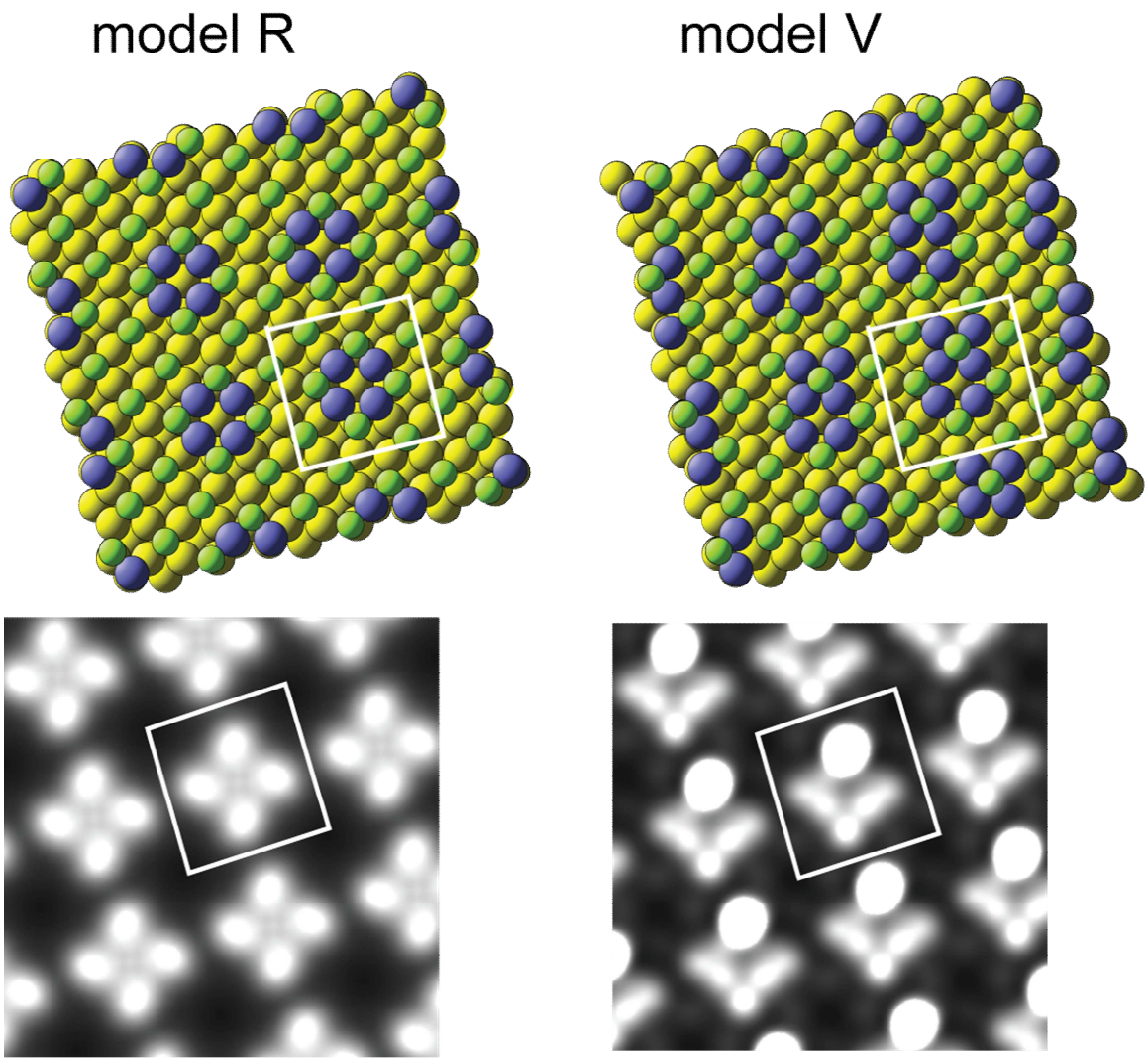

Fig. 4 Plan views of the two most favourable models of the Cu(100)(√17x√17)R14°-S surface, together with simulated STM images for these structures. The corresponding experimental STM image is shown in Fig. 3. For clarity the Cu atoms in the outermost (reconstructed) layer are shown in a different colour (blue) than the underlying bulk atoms (yellow/gold). The S atoms are represented by the smaller (green) spheres.

References

1 H.C. Zeng, R.A. McFarlane, K.A.R. Mitchell, Can. J. Phys. 68 (1990) 353.

2 E. Vlieg, I.K. Robinson, R. McGrath, Phys. Rev. B 41 (1990) 7896.

3 Q.T. Jiang, P. Fenter, T. Gustafsson, Phys. Rev. B 42 (1990) 9291.

4 A.E. Schach von Wittenau, Z. Hussain, L.Q. Wang, Z.Q. Huang, Z.G. Li, D.A. Shirley, Phys. Rev. B 45 (1992) 13614.

5 M.A. Van Hove, S.Y. Tong, J. Vac. Sci. Technol. 12 (1975) 230.

6 J.E. Demuth, D.W. Jepsen, P.M. Marcus, Phys. Rev. Lett. 31 (1973) 540.

7 J.L. Domange, J. Oudar, Surf. Sci. 11 (1968) 124.

8 D.P. Woodruff, J. Phys.: Condens. Matter, 6 (1994) 6067.

9 M.L. Colaianni, I. Chorkendorff, Phys. Rev. B. 50 (1994) 8798.

10 S.J. Clark, M.D. Segall, C.J. Pickard, P.J. Hasnip, M.J. Probert, K. Refson. and M.C. Payne, Z. Krist., 220 (2005) 567.

11 B. Hammer, L.B. Hansen, J.K. Norskov, Phys. Rev. B, 59 (1999) 7413.

12 J.P. Perdew, K. Burke, M. Ernzerhof, Phys. Rev. Lett. 77 (1996) 3865.

13 O.H. Nielsen, R.M. Martin, Phys. Rev. B 32 (1985) 3780.

14 M.J. Harrison, D.P. Woodruff, J. Robinson, Surf. Sci. 602 (2008) 226.

15 D. Sander, U. Linke, H. Ibach, Surf. Sci. 272 (1992) 318.

16 H. Ibach, Surf. Sci. Rep. 29 (1997) 195.

17 J. Tersoff, D.R. Hamann, Phys. Rev. Lett. 50 (1983) 1998.